Journal of Applied Polymer Science

The Preparation and Crystallization of Long Chain Branching Polylactide Made by Melt Radicals Reaction

Jinxiu You,[1] Lijuan Lou,[1,2] Wei Yu,[1] Chixing Zhou[1]

[1]Advanced Rheology Institute, Department of Polymer Science and Engineering, Shanghai Jiao Tong University, Shanghai 200240, People's Republic of China

[2]Petrochemical Research Institute, Petrochina, Beijing 100195, People's Republic of China

Correspondence to: W. Yu (E-mail: wyu@sjtu.edu.cn)

ABSTRACT: Long chain branching (LCB) of polylactic acid (PLA) was successfully prepared by melt radicals reaction with pentaerythritol triacrylate (PETA) and bis (1-methyl-1-phenylethyl) peroxide (DCP). The topological structure of the LCB was investigated by rheology and branch-on-branch (BOB) model was used to estimate the exact chain structures of the products, where comb-like LCB structures were generated due to the complex coupling between different macro-radicals. LCB structure was found to affect the crystallization of PLA products. In the temperature range of 110–130°C, the crystallization rate parameter (k) was improved sharply and the half crystallization time was decreased significantly after the grafting of PETA, which was ascribed to the enhanced hydrogen bonding in PETA-grafted long chain branching PLA. By comparing with the LCB PLA made from chain extension using multifunctional monomer, it shows that the crystallization becomes slower in a highly branched material with extremely long relaxation time if the effect of hydrogen bonding is similar. © 2013 Wiley Periodicals, Inc. J. Appl. Polym. Sci. 129: 1959–1970, 2013

KEYWORDS: addition polymerization; crystallization; structure–property relations; biopolymers and renewable polymers; rheology

Received 14 October 2012; accepted 29 November 2012; published online 3 January 2013
DOI: 10.1002/app.38912

INTRODUCTION

Recently, biodegradable polymers have received more and more attention. One of the most important biodegradable polymers is polylactic acid (PLA). PLA is an environmentally friendly polymer and it could be used as the traditional commodity plastics with the high mechanical properties, thermoplasticity, and biocompatibility.[1–3] However, because of hard and brittle mechanical properties of PLA, the practical application and development were limited.[1–3]

To expand the application range of the PLA, its physical and mechanical properties must be improved.[4,5] On the one hand, the melt strength of PLA is weak, which hinders its processing using elongation dominated flow, like film blowing. On the other hand, PLA is a slowly crystallizing material with low crystallinity, which requires a long processing cycle and restricts its practical application. Actually, different efforts have been made to improve melt strength and the crystallization separately. Several modifications have been made to improve the crystallizing properties of PLA. These attempts include changing the composition of polylactide random copolymers,[6–8] plasticization,[9–12] and blending of nucleating agent.[13–18]

Baratian et al. found that both crystallization rate and spherulite growth rate decreased significantly with increasing content of D-lactide.[6] James et al. investigated the crystallization behavior of polylactide random copolymers and stereochemical defects by time-resolved wide-angle X-ray diffraction and small-angle X-ray scattering (WAXD/SAXS) experiments.[7] On the other hand, various kinds of plasticizers including poly(propylene glycol) (PPG), poly(ethylene glycol) (PEG), and glycerol were used to improve the mechanical properties. Some authors found that PEG with molecular weight of 400 was an effect plasticizer to accelerate the spherulite growth rate of PLA.[9] Inoue et al. studied the blend of PLA and poly(butylenes succinate-*co*-L-lactate) (PBSL) with Rikemal PL710 (RKM) as plasticizer and further investigated the crystallization behavior. They found that crystalline growth rate was accelerated with addition of RKM.[10] Yeh et al. investigated neat PLA and plasticized PLA with triphenyl phosphate (TPP) and further discussed the crystallization kinetics.[11] The most frequently used nucleating agents include particles in nano-scale or micro-scale. For example, Liao et al.[14] investigated the isothermal cold crystallization kinetics of polylactide (PLA)/nucleating agents ($CaCO_3$, TiO_2, and$BaSO_4$) and found that crystallinity of PLA was increased. Besides the inorganic nucleating agent, there are organic nucleating agents, such as organic phosphate, carbon nanotubes.[15,16] Wang et al.[15] investigated the nucleation Rate of PLA composites with acid

oxidized carbon nanotubes of different aspect ratios and found that those with smaller aspect ratios enhance nucleation rate for PLA spherulites than those with larger aspect. Recently, some bio-based nucleators such as myo-inositol and TBC8-t were also reported. Kunioka et al.[17] found that isothermal crystallization of PLLA with 5 wt% myo-inositol at 100°C finished within 2 min after melting, while that of PLLA finished crystallization over 14 min under the same condition. Liang et al.[18] synthesized a novel nucleating agent TBC8-t and found that TBC8-t could greatly enhance crystallization rate of PLLA by increasing nucleation rate rather than crystal growth rate. Furthermore, crystallization peak temperature (T_c) and crystallization rate of PLLA nucleated with TBC8-t were much higher than that with conventional nucleating agent such as talc.

To improve the melt strength, an easy approach is to modify the chain topology, i.e., introduction of long chain branching into the materials. There are some literatures about melt radicals reaction of PLA with the presence of monomer and initiator, such as reaction of PLA with monomer maleic anhydride (MA) and peroxide.[19–21] These published researches usually focused on two aspects of the reaction: the first is influence factors of the melt free radicals reaction, such as peroxide, monomer content, and reaction temperature, and the second is speculation about the proposed reaction mechanism. Other method to introduce the long chain branching includes the chain extension reaction using multifunctional monomers,[22] which can form long chain branched structure with complex topology. Moreover, monomer trimethylolpropane triacrylate [TMPTA] was used to prepare LCBPLA by electron beam irradiation.[23,24] However, there is still a question that if both crystallization and melt strength can be modified simultaneously by controlling the chain structures. In this aspect, several studies have shown the effect of long chain branching (LCB) on the subsequent crystallization of polymers. An example is using the melt radicals reaction to produce branched polypropylene (PP) with pentaerythritol triacrylate (PETA).[25–27] Wang et al.[22] found that PETA grafted into PP and crystallization temperature were higher than that of the virgin and degraded polypropylenes. Tian et al.[26,27] investigated crystallization kinetics about linear and long chain branched PP. It was found that crystallization of PP increased with increasing concentrations of PETA. It was thought that LCB played as heterogeneous nucleating agent to improve performance of crystallization for PP.

Thus, in this article, our study is focused mainly on the crystallization behavior about grafted PLA sample by melt radicals reaction with PETA as monomer. We also try to compare its crystallization behavior with LCB PLA made from different approach. One purpose is to understand the reaction mechanism of radical reactions and the chain structure of grafted PLA. The other purpose is to understand the crystallization of LCB PLA, its dependence on the chain topology and its compositions.

EXPERIMENTAL

Materials

PLA was a NatureWorks® product 2002D. The content of L-lactide was about 96 wt% and the monomer was less than 0.3 wt%. The antioxidant Irganox 1330 was provided by Ciba, Switzerland. Pentaerythritol triacrylate (PETA) was obtained from Tianjin Kermel Chemical Reagent Co., Ltd, China. All were used as received without any further treatment. Dicumyl peroxide (DCP) was received from Shanghai Chemicals Factory, China, which must be purified and recrystallized for at least three times at room temperature to eliminate the influence of water.

Table I. Sample Name and Its Composition

Sample	DCP (%)	PETA (%)	1330 (%)
PLA	-	-	-
D1	0.3	-	0.2
D2	0.3	3	0.2

Sample Preparation

PLA was dried at 45°C for at least 24 h in vacuum before mixing. Grafted PLA samples were prepared by direct melt radicals reaction in a Rheomix-600 mixer (Haake Rheocord 90, Germany) using neat PLA with the monomer PETA and the radicals initiator DCP. Melt mixing was operated at 180°C. The rotor speed was initially set as 20 rpm during the addition of materials, and was later increased to 60 rpm for 10 min. The detailed compositions are listed in Table I.

A LCB-PLA made by chain extension using polyfunctional monomer is also used as a comparison. The sample is named as P-P02-T04, which contains 65 g PLA, 0.2 g pyromellitic dianhydride (PMDA), 0.4 g triglycidyl isocyanurate (TGIC), and 0.5 wt% 1330. PLA was melt reacted with PMDA first and then with TGIC. The details of sample preparation and structural analysis can be found in previous publication.[22]

Gel Determination and FTIR Spectroscopy

Before the characterization of Fourier transform infrared spectroscopy (FTIR), the gel content was tested. The samples were cut into pieces and packed with filter paper, which were Soxhlet extracted in boiling chloroform for 24 h. No insoluble portion was found in all the samples, which implies that no gel was formed.

For FTIR spectroscopy, the samples were dissolved in dichloromethane at room temperature and cast onto a thin KBr disk. The films were dried in a nitrogen chamber before the spectra were taken. The FTIR spectra were recorded with a Paragon 1000 FTIR spectrometer (PerkineElmer, Inc., USA). The samples were scanned in the appropriate range to detect the grafting reaction.

Moreover, variable temperature FTIR spectra of the grafted PLA were recorded to further investigate the effect of hydrogen bonding. The sample was heated from 25 to 180°C at the heating rate of 4°C/min and the FTIR spectra were recorded.

Rheological Measurement

Before the rheological measurement was performed, the samples were prepared by compression molding into sheets about 1 mm at 180°C under 10 MPa. Disks of 25 mm in diameter were cut from the sheets for rheological experiments. The linear

viscoelastic tests were carried out on a rotational rheometer (Bohlin Gemini 200HR, Malvern Instruments, UK) with parallel plate geometry of 25 mm in diameter and a gap of about 1 mm. The dynamic time sweep tests were first performed at 1 Hz and 180°C with the stain amplitude of 1% to check the stability of samples. The critical strain amplitude for the linear viscoelastic region of pure PLA is about 20%, and in the range of 10% for grated samples at 1 Hz and 180°C. Then, the small amplitude oscillatory shear (SAOS) was applied and the dynamic frequency sweep was carried out. The range of the frequency sweeps was from 0.01 to 100 rad/s at constant strain amplitude of 5%.

Differential Scanning Calorimetry (DSC) Analysis

The thermal characteristics and crystallization behavior of different PLA samples were studied with a differential scanning calorimeter (DSC, A Perkin-Elmer PYRIS) in a nitrogen atmosphere.

About 6 mg samples were weighed for DSC tests. For the first scan, it was heated from 25 to 200°C at the heating rate of 10°C/ min, and hold for 3 min to eliminate thermal history. Then it was cooled to 25°C at the same speed and held for 3 min. Finally, the sample was heated again to 200°C at 10°C/ min. The cold crystallization temperature (T_c), the glass transition temperature (T_g), and the melting temperature (T_m) of neat PLA and grafted PLA were measured in the second heating scan.

For isothermal cold crystallization, the sample was heated from 25 to 200°C at 10°C/min and held for 3 min. Then it was cooled to 25°C at the same speed, and held for another 3 min. Finally, it was heated at 100°C/min to a certain temperature (110–130°C in this work) for crystallization.

Polarized Optical Microscopy (POM) Analysis

A Polarizing Optical Microscope (Leica DMLP, LECIA Corp., Germany) equipped with a programming temperature controller (TMS 94, Linkam Scientific Instruments Ltd, U.K.) and a Sony digital camera was used to investigate crystals morphologies of PLA samples. Neat PLA and grafted PLA were placed between two microscope cover glasses, and heated at a rate of 50°C/min to 200°C from room temperature, held at 200°C for 5 min. Then it was rapidly cooled down to a preset crystallization temperature (T_c) between 115 and 130°C. The growth of spherulites was observed and recorded.

Wide-Angle X-ray Diffraction (WAXD) Analysis

WAXD analyses for neat PLA and grafted PLA were obtained using an X-ray diffract meter (Rigaku, Japan) by Cu Kα radiation ($\lambda = 0.154$ nm) at a voltage of 80 kV and a current of 20 mA. The PLA samples were scanned at room temperature at the scanning speed 4°/min with the diffraction angle (2θ) in the range of 5°–40°.

RESULTS AND DISCUSSIONS

FTIR Spectroscopy

Figure 1 shows the FTIR spectra of neat PLA, PETA, and grafted PLA (D2) samples. The grafted PLA (D2) was purified and the possible residual PETA during mixing was removed. The characteristic peak of PLA is very clear.[28–30] For example, the strongest band observed at 1760 cm^{-1} was C=O stretching mode, the double bands at 2945 and 2996 cm^{-1} were assigned to ν_{as}-CH_3 stretching mode, and the band at about 865 cm^{-1} was the characteristic peak of C—COO stretching mode in neat PLA polymer.

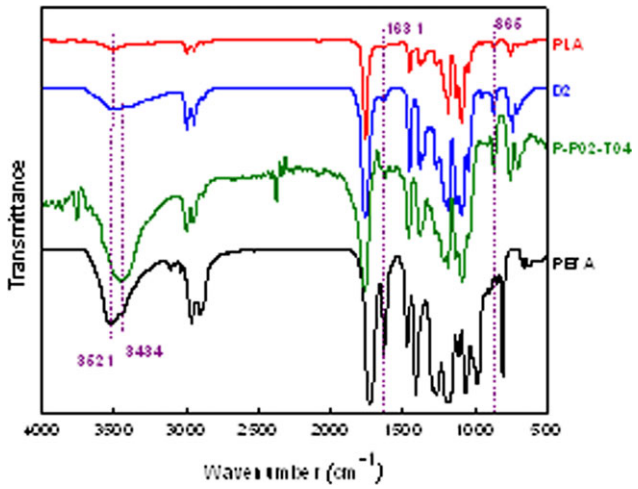

Figure 1. FTIR spectra of neat PLA, PETA and purified grafted PLA D2. [Color figure can be viewed in the online issue, which is available at wileyonlinelibrary.com.]

A new band appears at about 1631 cm^{-1} in the D2 sample, which is absent in neat PLA polymer in the range of 1620–1647 cm^{-1}. Such absorption is ascribed to the stretching mode of C=C and clearly seen in PETA. It implies that PETA has been grafted onto the PLA chains successfully. The absorption band centered at 3504 cm^{-1} is attributed to the end hydroxyl group of the PLA.[30] For PETA, the absorption band of hydroxyl group is strong at 3521 cm^{-1}. The peak is broad to show a shoulder at 3434 cm^{-1} due to the intermolecular hydrogen bonding between hydroxyl group and carbonyl group.[31] When comparing PLA and grafted PLA (D2), the characteristic peak of hydroxyl group in D2 was shifted to lower wavenumber and became broader. Such shifts are similar to that in PETA, and usually related to the formation of hydrogen bonding. It indicated that the grafted PETA on PLA promotes the formation of hydrogen bonding between PLA molecules. Similarly, the hydrogen bonding is also seen in P-P02-T04 sample, and the hydrogen bonding is expected to be stronger than that in D2 if the strength of the peak at 3504 and 3434 cm^{-1} are compared. The strong hydrogen bonding in P-P02-T04 is due to the large amount of hydroxyl group and carboxyl group after PLA reacted with PMDA and TGIC.[22]

To further discuss the intermolecular hydrogen bonding of D2, FTIR under variable temperatures were performed and shown in Figure 2. At room temperature, the hydroxyl absorption peak is at 3494 and 3434 cm^{-1}, which is a wide absorption peak. The adsorption peak at lower wavenumber is attributed to the hydrogen bonding between the molecules. The hydrogen bonding can be formed between the end carboxyl or hydroxyl group of the PLA and the carbonyl of PETA, or the hydroxyl group of

Applied Polymer SCIENCE

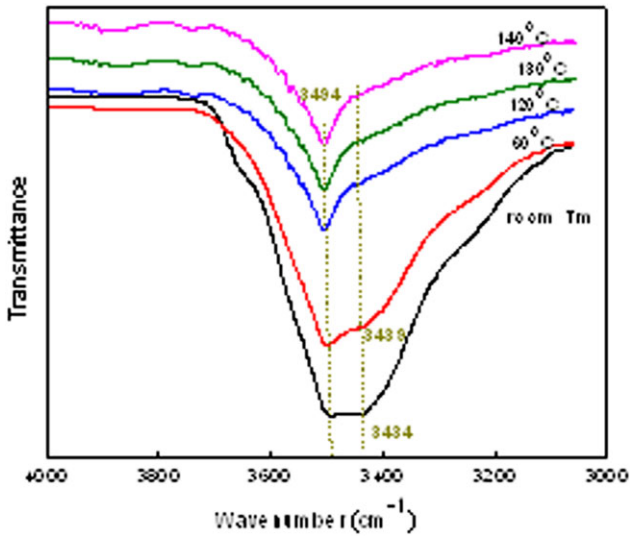

Figure 2. FTIR spectra of D2 sample under different temperatures. [Color figure can be viewed in the online issue, which is available at wileyonlinelibrary.com.]

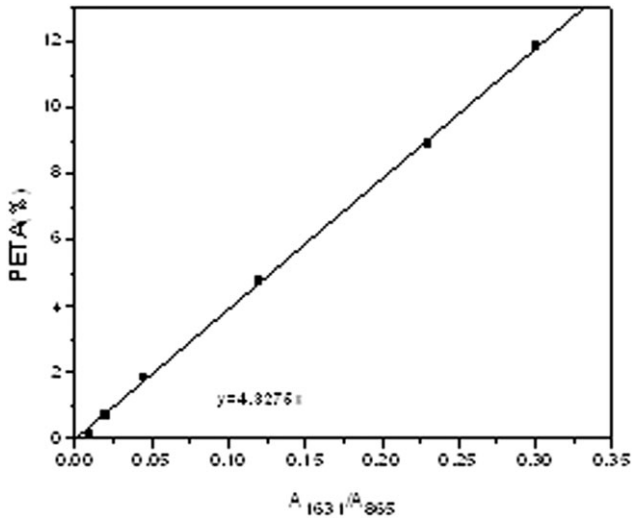

Figure 3. Calibration curve for the determination of reacted PETA in PLA-g-PETA.

the PETA and the carbonyl of PLA. As the temperature increases, the absorption peak due to hydroxyl group becomes narrower, and the shoulder at 3434 cm^{-1} gradually moves to high wavenumber and becomes weaker. When the temperature is higher than 120°C, the peak initially at 3434 cm^{-1} almost disappeared, and the peak becomes a narrow one and independent of temperature. This is attributed to weakened intermolecular hydrogen bonding with increasing temperature. Therefore, grafting PETA on PLA chain will not only functionalize the PLA chain, but introduce evident hydrogen bonding between PLA chains.

To get the monomer degree of branching (%), the standard curve is drawn using this followed equation 1:

$$\mathrm{BDI} = A_{1631}/A_{865} \quad (1)$$

BDI is double bond of the index. A_{1630} is the area of the absorption peak at 1631 cm^{-1}, representing the C=C in the PETA molecule. A_{865} is the area of the absorption peak at 865 cm^{-1}, representing the νC—COO stretching mode in the bond chain of PLA molecule. Then, a series of the certain amount of PETA monomer and PLA polymer were blended in a Rheomix-600 mixer. The condition is same as mentioned in sample preparation. These FTIR spectroscopies of the samples are characterized and the standard curve was got with the equation 1, as shown in Figure 3. The degree of branching of D2 is about 0.9%.

Rheological Properties

It has been shown that radial reaction in melt can introduce long chain branching in polymer molecules.[14,26] Among all the possible methods to find out if there exists long chain branching, rheological methods are found to be quite simple and effective. The principle is the appearance of long relaxation time due to the change in the topology of molecules. For linear polymers, the typical terminal flow behavior can be observed in the dynamic storage modulus (G') and loss modulus (G''), i.e., $G'\alpha\omega^2$ and $G''\alpha\omega$, which is a characteristic of viscoelastic liquid. The dynamic moduli of neat PLA and grafted PLA are shown in Figure 4. It is clear that neat PLA exhibits the typical terminal flow behavior at low frequency. For the grafted PLA samples D1 and D2, although the enhancement in G″ is limited, there are great increase in the storage moduli. D1 shows slight different behavior with a longer relaxation process at lower frequency as compared with neat PLA, indicating the possible formation of branched chains. With the addition of PETA, the terminal slope of G' of D2 is significant decreased in comparison with that of neat PLA and D1. The non-terminal behavior of D2 indicates the appearance of certain longer relaxation process that does not exist in linear PLA, which can also be ascribed to the long chain branches formed from the melt radicals reactions. Moreover, it is expected that the degree of LCB or the

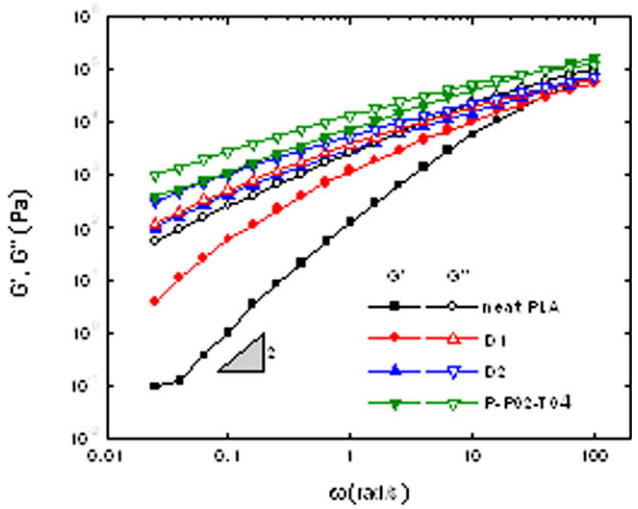

Figure 4. Storage modulus vs. frequency for PLA, D1, and D2 samples at 180°C. [Color figure can be viewed in the online issue, which is available at wileyonlinelibrary.com.]

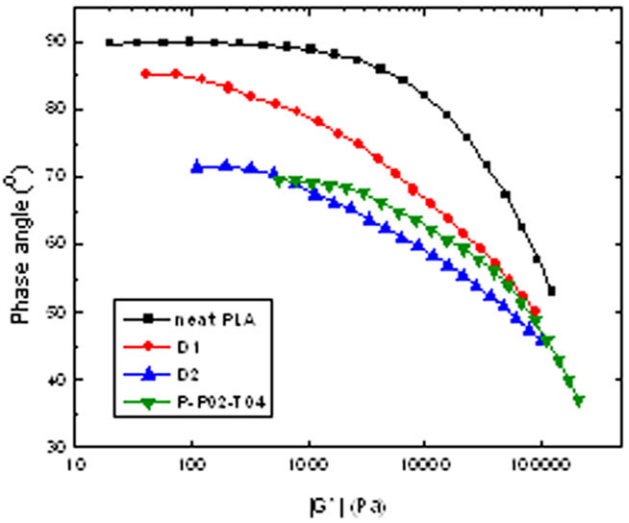

Figure 5. van Gurp-Palmen plot of PLA, D1, and D2 samples at 180°C. [Color figure can be viewed in the online issue, which is available at wileyonlinelibrary.com.]

chain topology of D1 molecule and D2 molecule should be quite different, which explains the evident difference in storage moduli in D1 and D2. The dynamic moduli of P-P02-T04 sample are also shown in Figure 4 for comparison. It is evident that its G' and G'' are higher than that of D2, which implies that either the P-P02-T04 sample has a higher molecular weight or has a higher level of long chain branch.

The other frequently used method is the so-called van Gurp-Palmen (vGP) plot, which was suggested to check the validity of time-temperature superposition principle and found later sensitive to the branched structure of polymer chains. It is done by plotting the phase angle (δ) versus complex modulus ($|G^*|$) for the polymer systems. The vGP plots of three PLA samples are shown in Figure 5. All the phase angles decrease with the increase of complex modulus. The minimum of phase angle that corresponds to the plateau modulus is not observed here due to the limited data at high frequency. As the complex modulus decreases, the phase angle of neat PLA quickly goes to 90°, which correspondences to the viscous terminal behavior. For two branched samples D1 and D2, the deviation from the linear PLA is obvious. The phase angle of D1 and D2 does not reach 90° in the experimental range of frequency, which implies that the relaxation time of them would be much larger than the reciprocal of the lowest frequency (0.01 rad/s) in experiments. The phase angle of P-P02-T04 lies between D1 and D2 at the same complex modulus. Generally, the decrease in phase angle can be ascribed to the wide distribution of molecular weight[32] or the long chain branching in polymer chains.[33] The change of polydispersity during melt radicals reaction is possible for PLA, but its variation is not expected to be significant. Then, the low phase angle at constant complex modulus suggests a higher elasticity, which in this work could be attributed to the long chain branching. It is expected that D2 sample has a larger degree of LCB than D1 due to the lower phase angle in D2. Therefore, it is believed that the melt reaction with the addition of DCP in PLA can cause long chain branching, while melt radicals reaction with the presence of PETA can further increase the level of LCB. However, direct comparison of the long chain branch level in D2 and P-P02-T04 is not easy from vGP plot since both the branch level and the chain topology will affect the phase angle.[22]

Chain Topology and Possible Reaction Mechanism

Although the existence of long chain branching is evident from the linear viscoelasticity as shown above, quantitative analysis on the level of branching or the chain topology is still difficult. Trinckle et al.[33] had tried to setup a topology map, which took use of the vGP plot to classify the topology of branched polymers from transition points (the inflection point or local minimum point) of phase angle. However, it has been shown recently that such method is not unique even for monodispersed model branched polymers.[34] In some cases, additional information like molecular weight and its distribution are needed for separate polymers with different topologies but similar transition points. In polymers with polydispersity in molecular weight and chain topology, it is unknown if such simple topology map still exists or not. Instead, fitting the dynamic moduli with the molecular model seems to be a feasible approach.[33] The branch-on-branch (BOB) model based on molecular dynamics is one of the most successful models to predict the linear viscoelasticity of polymers with different topological chain structures, such as H-type, symmetric-star, asymmetric-star, comb, and tree-like.[35] By fitting the experimental data such as dynamic modulus, phase angle, and complex viscosity, the BOB model is able to determine the compositions and chain structures of samples with the model predictions. In our previous study,[22] the BOB model was used to investigate the PLA samples produced from end group reactions and the compositions and chain topologies of the products were predicted successfully. In this work, the BOB model was also applied to predict the chain structures of different products obtained from melt radicals reaction. The molecular parameters are the same as those used previously,[22] i.e., the number of repeating unit in one entanglement segment is 110 and the entanglement time is 10^{-5}s at 180°C. First, the fitting for the linear PLA is applied. It is shown in Figure 6(a) that the best fit can be obtained for linear PLA with the weight average molecular weight (M_w) 102 kg/mol and the polydispersity index (PDI) 1.2 at 180°C. This justifies the consistency of the current data with our previous study.

Then, the linear viscoelasticities of D1 and D2 were fitted by the BOB model. The fitting results for D1 and D2 are shown in Figure 6(b,c). The fitting lines for dynamic moduli and complex viscosity are generally satisfactory, with only a slight deviation in the phase angle. The parameters used to fit linear viscoelasticity and possible chain structures for linear PLA, D1, and D2 samples are listed in Table II, where φ stands for volume fraction of the corresponding component, M_a and M_b are the molecular weight of arm and backbone in the unit kg/mol, respectively. It can be seen that the components of D1 include linear chains and small amount of comb-like chains with less than three arms. The molecular weight of linear chains in D1 is smaller than the original linear PLA, which implies the degradation of PLA chain during melt radicals reaction. The backbone

Applied Polymer SCIENCE

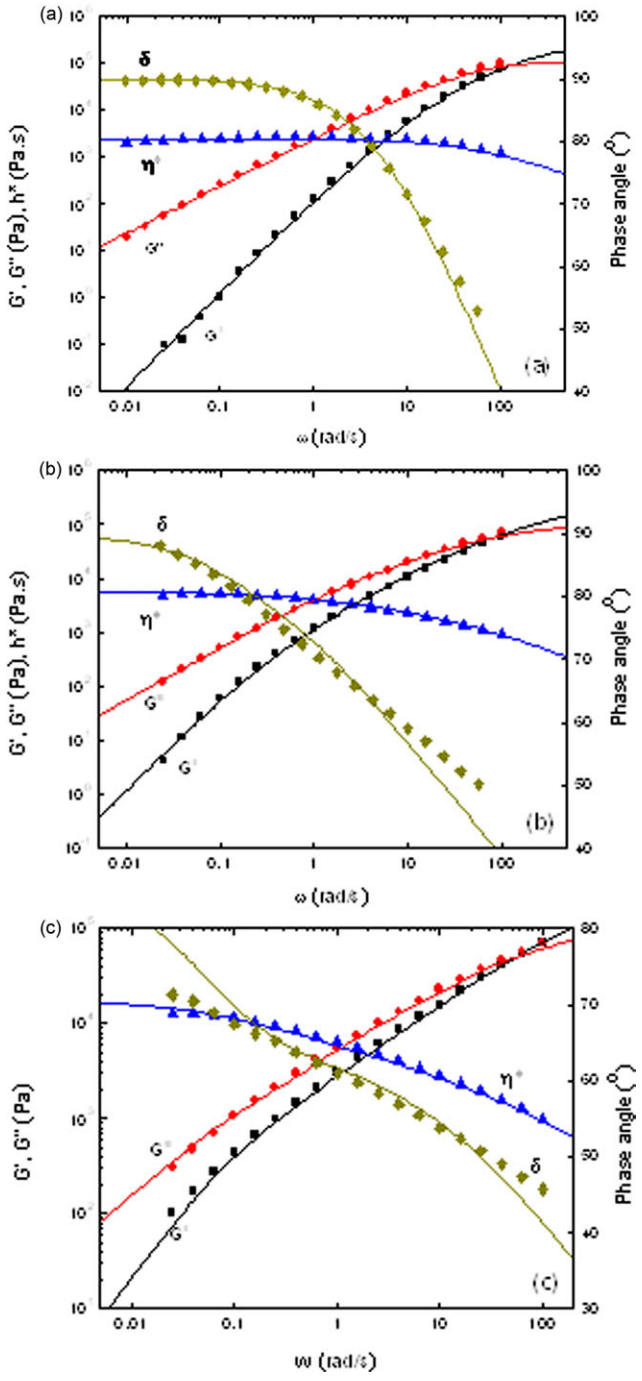

Figure 6. Linear viscoelastic spectra at 180°C for neat PLA (a) D1 (b) and D2 (c) (scatters are the experimental data, and lines are the predicted results of BOB model). [Color figure can be viewed in the online issue, which is available at wileyonlinelibrary.com.]

length of the comb-like chain in D1 is about twice of the linear chain, which suggests that the backbone of comb-like chain might be the coupling product of two linear chains. D2 sample is also composed of linear chains and comb-like chains. The molecular weight of linear chains in D2 is also similar to that of D1, which implies that the addition of PETA does not reduce the degradation. Instead, the decrease in the fraction of linear chains suggests that PETA can promote the formation of branched chains. Moreover, the comb-like chains in D2 is composed of a shorter one and a longer one, with the structure of the former similar to that in D1, which is generated purely due to the radicals reaction initiated by DCP. The longer comb in D2, however, reflects the additional reaction with the grafted PETA.

The compositions and chain topology of P-P02-T04 sample[22] are also listed in Table II as a comparison. Unlike the product from free radical reactions, P-P02-T04 is composed by linear chains, star-like chains, and tree-like chains. The arm of star-like chains has the same length as the linear ones, which implies its formation through a monomer (such as TGIC) with three functional groups. The tree-like chains have two generations with a three-arm star core. The molecular weight of tree-like molecules is rather large and the complete relaxation requires quite long time. Actually, it has been shown by the creep tests[22] that the terminal regime of P-P02-T04 sample appears at 10^{-4}rad/s, much lower than that of D2 sample.

For D2, by above-mentioned FTIR spectra analysis, it was known that the monomer PETA grafted on the polylactic acid. The LCB structures in final products are attributed to the coupling between macro-radicals, and the grafted PETA can also be involved in such reaction to cause a high level of branch. Besides the melt radicals graft reaction, the chain scission reaction of PLA easily happened under heating conditions. Therefore, the melt radicals reaction mechanism is suggested.[19,21,36]

As shown in Scheme 1, there are free radicals in the backbone of PLA (a) after the hydrogen radicals abstraction reacted. Because this kind of free radicals is not stable, the chain scission easily happened to create more stable of free radicals as (b).[36] Then, the macro-radicals (b) can react with PLA chains to obtain the grafted product (I) which is the main grafting reaction between PLA and DCP as shown in reaction (1). So D1 sample is made of linear PLA including the chains by chain scission and a few comb-like chains. Compared with PLA, the radicals branching reaction between the chain (b) and PETA is more likely to happen because of the higher activity of C=C. As shown in reaction (2), the primary product of (c) with different structure was generated. These products could be degraded linear chains, the chain-extended linear chains using PETA and branched chain with PETA as the branching kernel. These grafted chains can further reaction with macroradicals like (b) to form branched chains with more branching points. Actually, the topology of branched chain could be much more complex. However, fitting the rheological data with the BOB model suggests that D2 sample is probably to contain linear PLA chains (c), comb-like chains (I) comb and (II) comb with side arms more than 3. The content of longer comb in the sample depends on the amount of PETA and the reaction conditions.

Crystallization Behavior

Figure 7 showed the second heating behavior of neat PLA and grafted PLA at the scanning rate of 10°C/min after eliminating the thermal history. For neat PLA, the glass transition temperature is about 57°C and there is a very weak cold crystallization

Table II. Parameters Used to Fit Linear Viscoelasticity for PLA Samples

	Component I: linear chain		Component II: comb-like chain		
	φ_{linear}	M_w/PDI	φ_{comb}	M_b/PDI	M_a/PDI
PLA	1.00	102/1.2	-	-	-
D1	0.72	80/1.4	0.28	160/1.1	80/1.1 (q = 2.5)
D2	0.66	80/1.4	0.12	160/1.5	80/1.5 (q = 3)
			0.22	320/1.5	80/1.5 (q = 6)
P-P02-T04[20]	0.60	110/1.2	φ_{star} = 0.25		110/1.2
			φ_{tree} = 0.15		$M_{g,0}$/PDI = 50/1.0
					$M_{g,1}$/PDI = 220/1.0

peak at about 134°C. The total degree of crystallinity is less than 1% in neat PLA, which is consistent with previous studies that commercial PLA is hard to crystallize due to the small amount of D-lactide. After melt radicals reaction initiated by DCP, there was a shift in exothermic peak on the heating curve. It means that more crystals were formed in the process of heating. When the PETA is involved in the radicals reactions, a pronounced cold crystallization peak appears where the peak of crystallization shifts to even lower temperature. The data of the glass transition temperature (T_g), the cold crystallization temperature (T_c), and the melting temperatures (T_m) were listed in Table III. It is clear that the crystallinity, glass transition point (T_g), and melting point (T_m) are all influenced by the branched structure of grafted PLA. Introduction of branched structure by DCP only slightly improves the cold crystallization by decreasing the crystallization temperature, while additional branching using PETA causes further decrease in the crystallization temperature. P-P02-T04 sample shows the lowest crystallization temperature. Meanwhile, the melting point decreases when there is long chain branching in PLA, which is ascribed to the imperfect crystal structure during the faster crystallization in the branched PLA. There is no difference between the melting points of D2 and P-P02-T04. The major difference between branched PLA made by different approaches is the degree of crystallinity. The cold crystallization of P-P02-T04 during second heating is greatly enhanced as seen from ΔH_c. However, the crystallinity of P-P02-T04 during cooling as calculated from the difference between ΔH_m and ΔH_c is still similar to the neat PLA, which implies the branched structure in P-P02-T04 does not contribute to the crystallization during cooling. D2 sample, on the other hand, not only promotes the cold crystallization during the second heating, it also increases the crystallinity during cooling to about 13%. The promotion of cold crystallization in D2 and P-P02-T04 is possible related to the hydrogen bonding formation in these branched polymers. However, the extremely long relaxation process in P-P02-T04 implies that its chain mobility is much smaller than that of D2, which slows

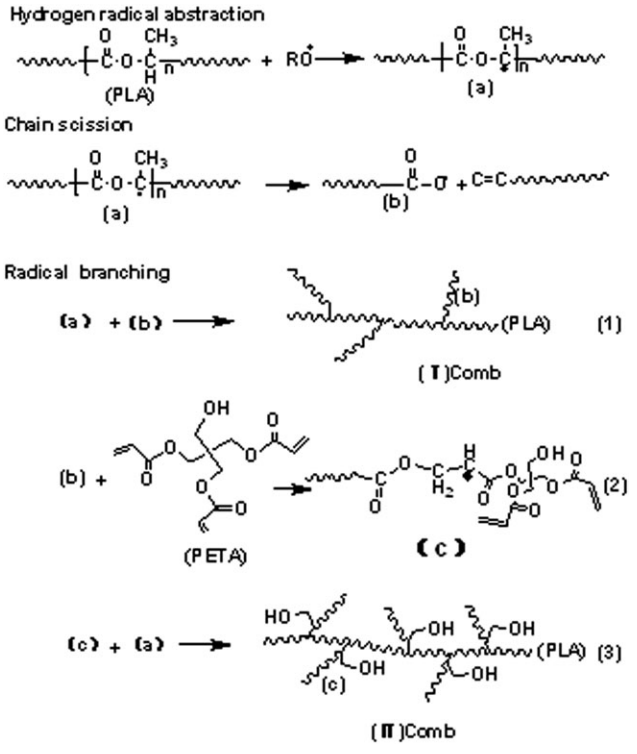

Scheme 1. The proposed reaction mechanism about the melt radicals reaction of PLA with PETA and DCP.

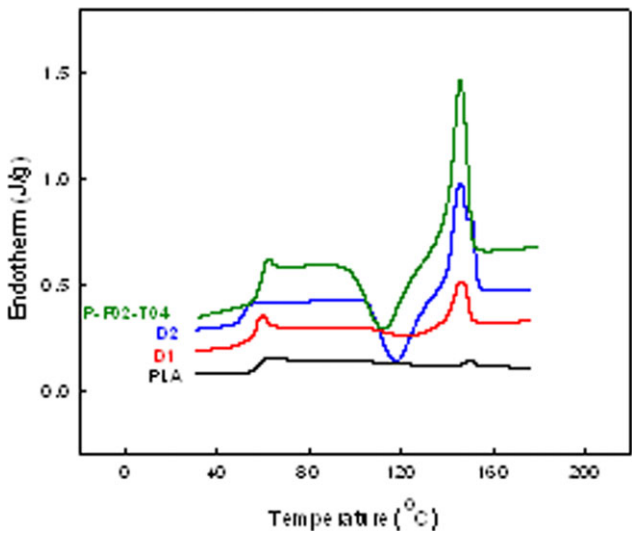

Figure 7. The second heating curves of PLA, D1, and D2 samples at 10°C/min scanning rate. [Color figure can be viewed in the online issue, which is available at wileyonlinelibrary.com.]

Table III. Results from the Thermal Analysis of the Neat PLA and Grafted PLA

Sample	T_g (°C)	$T_{c,peak}$ (°C)	T_m (°C)	$-\Delta H_c$ (J/g)	ΔH_m (J/g)	X_c[a] (%)
PLA	57.1	134	150	0.07	0.88	0.94
D1	55.8	122	146	2.13	5.38	3.47
D2	52.5	117	145	12.6	24.8	13.0
P-P02-T04	60.8	113	145	19.0	20.3	1.41

[a] X_c (%) = 100 × ($\Delta H_c + \Delta H_m$)/ΔH_{m0} with ΔH_{m0} = 93.7 J/g[38] for PLA.

down the crystallization process during cooling. The fact that branched structure can affect the thermal behavior has also been observed in some publications. Ohya et al.[37] reported a lower glass transition temperature (T_g), melting temperature (T_m) in branched poly (lactide) (PLA) with various lengths of graft chain. However, our results imply that the glass transition temperature might be related to the level of branch as well as the topology of molecules.

Wide-angle X-ray diffraction (WAXD) was used to investigate the crystalline structure of PLA samples. The diffraction patterns of PLA quenched directly from melt state are shown in Figure 8(a). It is clear that PLA and D1 show broad peak without annealing, which implies that neat PLA and D1 are in amorphous state after cooling. P-P02-T04 sample is also in amorphous state from the broad peak in WAXD. This is consistent with that DSC test that crystallization is difficult in P-P02-T04 sample during cooling. However, D2 presents clear diffraction peaks as shown in Figure 8(a), which means that the D2 sample is well crystallized even under quick quench. The peaks appeared at the 2θ values of 14.8°, 16.7°, 19.2°, and 22.3°, which were ascribed to the (010), (110/200), (203), (015) reflection, respectively. Three peaks of which at 2θ = 16.7°, 19.2°, and 22.3° are the characteristic peaks of α-form PLA, and 2θ = 14.8° and 19.2° are characteristic peaks of β-form crystal.[39] After the samples were annealed for 1 h at 110°C, the results of WAXD patterns for PLA, D1, D2, and P-P02-T04 at room temperature were shown in Figure 8(b). PLA, D1, and P-P02-T04 samples show clear diffraction peaks after annealing at 110°C. It was seen that the diffraction patterns of all samples are similar after annealing except that the 010 peak and 203 peak of β-form crystal are much weaker in neat PLA and D1. Therefore, both D2 and P-P02-T04 are characterized by α-form crystal with a very small fraction of β-form crystal, suggesting that branching structures do not change the main crystal structure of PLA. The higher crystallinities in D2 and P-P02-T04 are not caused by the change of the crystalline structure.

The kinetics of isothermal cold crystallization of linear and branched PLA is studied using DSC by heating the samples rapidly from the room temperature to the crystallization temperature T_c. The relative crystallinity X_t at different crystallization time can be obtained from the integration of the heat flow and a typical result is shown in Figure 9. The increase of crystallization speed after the grafting reaction is evident, where a slight decrease the half crystallization time ($t_{1/2}$) is observed in D1 as compared to neat PLA, while $t_{1/2}$ of D2 becomes much smaller than neat PLA. The half crystallization time of P-P02-T04 is between that of D1 and D2. Considering the possible change of equilibrium melting point after the change in the chain topology, a comparison of the half crystallization time at different degree of undercooling is shown in Figure 10. The degree of undercooling of PLA samples is defined as $\Delta T = T_m^0 - T_c$, where T_m^0 is the equilibrium melting point and T_c is crystallization temperature. The equilibrium melting point can be obtained from the intersection of the melting temperature-crystallization temperature line with the line $T_m = T_c$ in the Hoffman and Weeks plot. For neat PLA, D1, D2, and P-P02-T04, the equilibrium melting point temperature obtained was 162, 161, 158, and 159°C, respectively. From Figure 10, it is clear that the crystallization becomes faster as temperature decreases which is ascribed to the larger undercooling at lower temperatures.

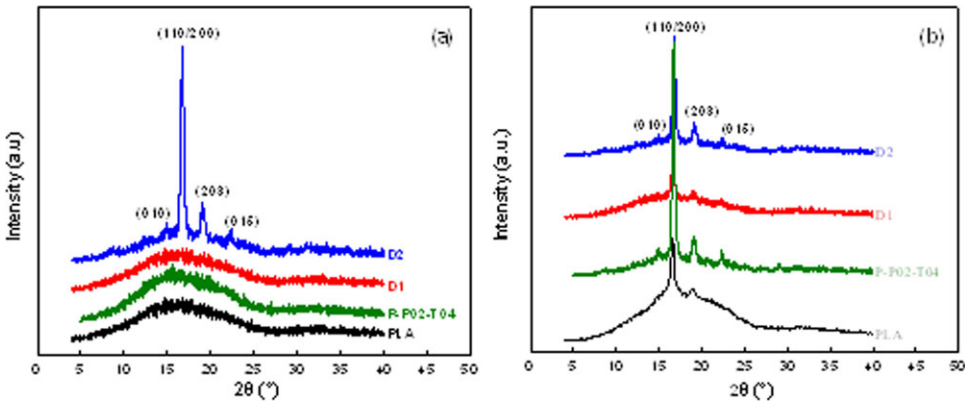

Figure 8. WAXD patterns for PLA, D1, and D2 without annealing (a) and after annealing at 110°C for 1 h (b). [Color figure can be viewed in the online issue, which is available at wileyonlinelibrary.com.]

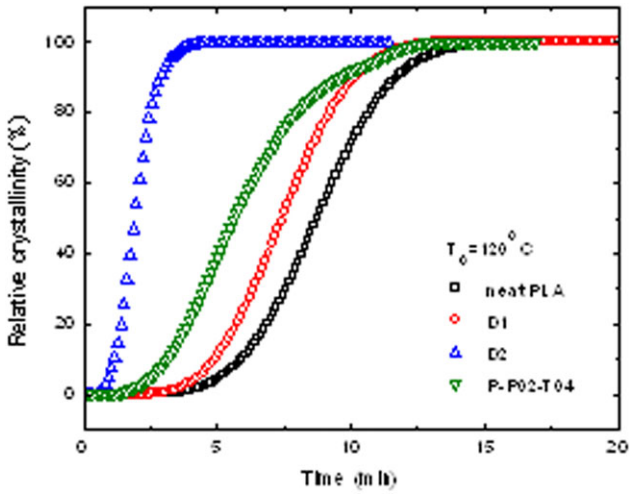

Figure 9. Relative crystallinity X_c of samples versus crystallization time for PLA, D1, and D2 at isothermal crystallization temperature 120°C. [Color figure can be viewed in the online issue, which is available at wileyonlinelibrary.com.]

Introduction of long chain branched structures in D1 only slightly decreases the half crystallization time of PLA under the same undercooling, while the significant decrease is seen in D2. Considering that the fraction of branching chains in D2 is only slightly larger than that in D1, it implies that the fast crystallization in D2 maybe not only ascribed to the branched structures. The half crystallization time of P-P02-T04 also decreases greatly as compared to the neat PLA, but its crystallization is still slower than D2.

In this study, the Avrami equation was used to analyze the isothermal crystallization kinetics of PLA samples, which can be expressed as:

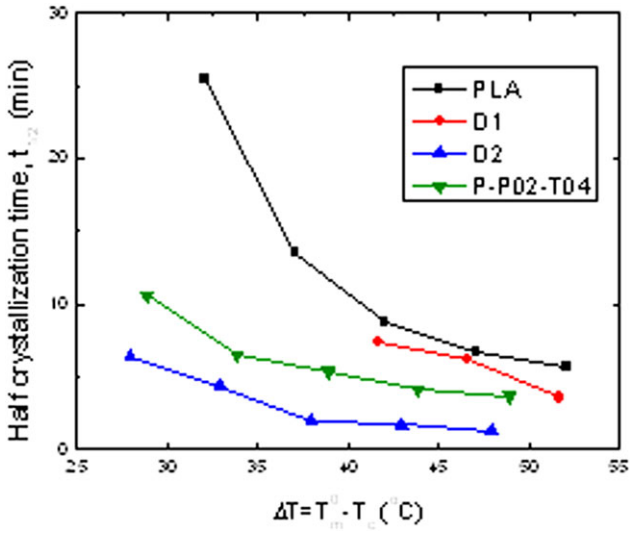

Figure 10. Half crystallization time under different degree of undercooling for neat PLA, D1, and D2. [Color figure can be viewed in the online issue, which is available at wileyonlinelibrary.com.]

Table IV. Avrami Parameters of the Neat PLA and Grafted PLA at Different Isothermal Crystallization Temperatures

sample	T_c (°C)	n	K (min^{-n}) × 10^5	$t_{1/2}$ (min)
PLA	110	4.5	30.9	5.66
	115	4.5	13.8	6.70
	120	4.5	4.17	8.75
	125	4.5	0.59	13.6
	130	4.6	0.02	25.4
D1	110	3.7	602	3.55
	115	3.8	66.4	6.26
	120	4.1	18.3	7.44
D2	110	3.8	17782	1.29
	115	3.2	13489	1.67
	120	3.5	7244	1.92
	125	3.9	199	4.32
	130	4.0	47.9	6.35
P-P02-T04	110	3.8	532	3.66
	115	3.3	664	4.12
	120	2.6	816	5.38
	125	2.8	375	6.52
	130	2.0	498	10.6

$$1 - X_t = \exp(-kt^n) \quad (2)$$

where X_t is the relative degree of crystallinity at time t, the exponent n is a constant depending on the type of nucleation and the growth dimension, and k is the crystallization rate constant associated with both nucleation and growth contributions. The Avrami parameters n and crystallization rate k can be obtained from the plots of $\ln[-\ln(1 - X_t)]$ versus $\ln t$, and the data were listed in Table IV.

The average value of n was around 4.5 for neat PLA polymer, 3.9 for the D1 polymer, and 3.7 for D2 polymer, while P-P02-T04 has a relatively smaller value of n. For neat PLA, similar Avrami exponent n has been reported in literatures.[28] For D1 and D2, the Avrami exponents n are in the range of 3–4, indicating that the microstructure and crystalline growth of D2 sample are still similar to that of neat PLA, but branched structure formed after radicals reaction may slightly decrease the exponent n. For the value of crystallization rate constant k, it decreases with the increasing crystallization temperatures (T_c) as shown in Table IV. Moreover, compared with neat PLA, the value of k of D2 is greatly increased with around 1000 times at the same crystallization temperatures (T_c). It indicates that the branched structure and PETA will significantly enhance the crystallization rate.

Generally, there are two factors that affect the crystallization of polymer. One is the nucleation density of spherulites and the other is the spherulitic growth rate. The half crystallization time and the crystallization rate constant k only give an overall evaluation of the crystallization speed. Figure 11 shows the spherulitic morphologies of the neat PLA, D1, and D2 using polarized optical microscopy during isothermal crystallization at 130°C.

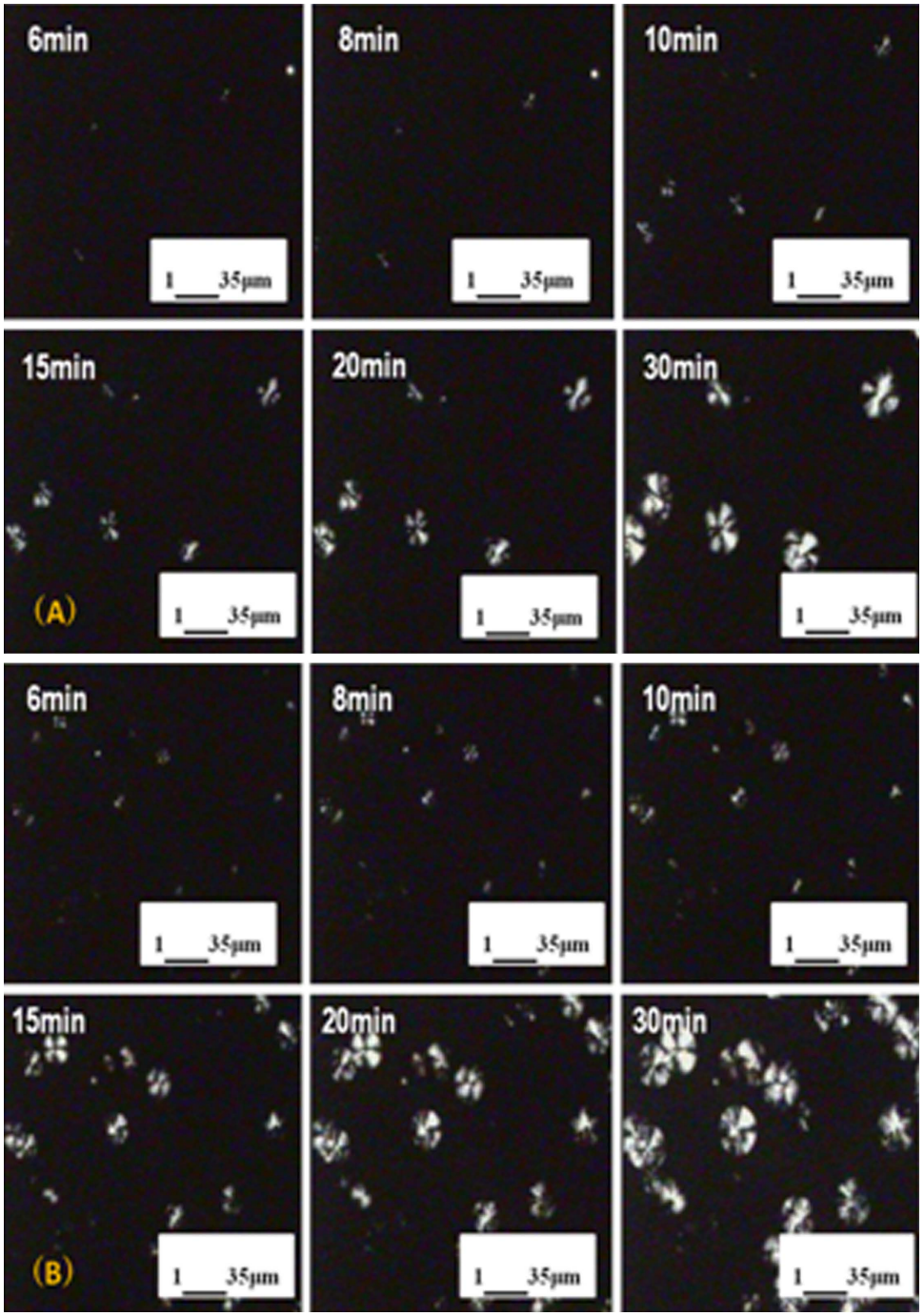

Figure 11. The morphology of spherulite for neat PLA (A), D1 (B) and D2(C) crystallized isothermally at 130°C at different time. [Color figure can be viewed in the online issue, which is available at wileyonlinelibrary.com.]

The spherulite is characterized by the Maltese Cross for all samples. On the one hand, the spherulitic growth rate for neat PLA, D1, and grafted PLA D2 polymer is calculated from the time-dependent size of spherulite. The spherulite of PLA and D1 shows a linear growth in the diameter with time at a growth rate 1.08 and 1.32 μm/min, respectively, while the spherulitic growth rate of D2 is 1.4 μm/min. The growth rate in D2 is slightly higher than that of neat PLA and close to that of D1, which could be ascribed to the increased chain mobility of linear chain in D2 sample due to the degradation during melt radicals reaction.

On the other hand and more importantly, it is obvious that there are more nuclei of spherulites for D2 than that of neat PLA and D1. The nucleation density of D2 is about 10 times as much as that of neat PLA. For D1, the nucleation density is only increased slightly as compared to that of neat PLA. Therefore, the main factor to accelerate the crystallization of D2 is

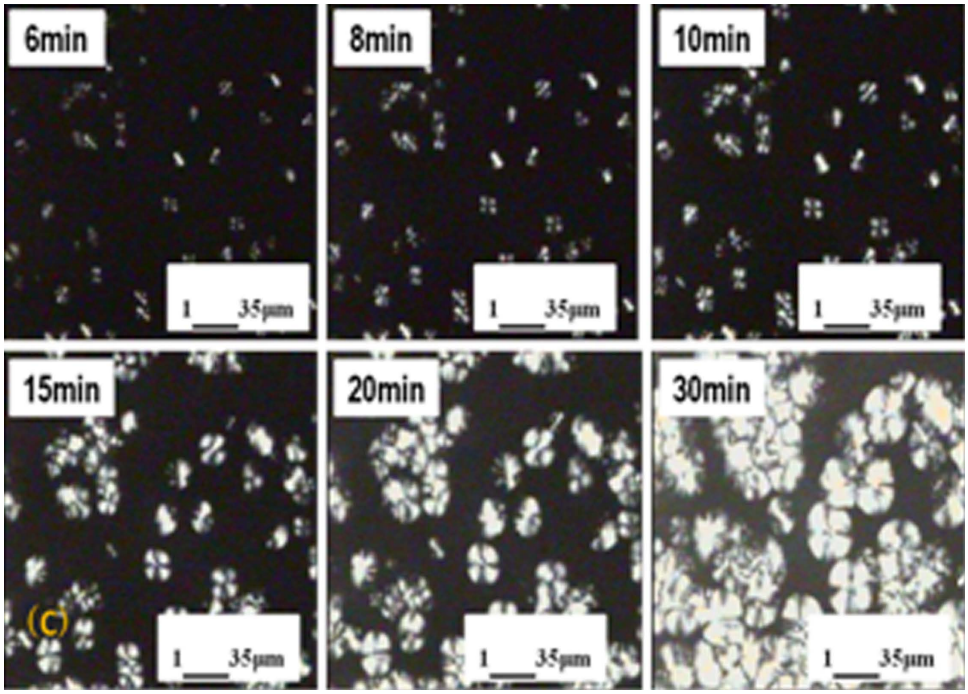

Figure 11. continued

the increase in the nucleation density. Some studies suggested that certain chemical bonds can affect the crystallization of polymer.[30,40] For example, the three-dimensional heterogeneous hydroxyl existed in some nucleating agent as nucleation to affect the polymers crystallization.[30] In our case, after the melt free radicals reaction with the monomer PETA and initiator DCP, the product has intermolecular hydrogen bonding formed from between —OH in side arms and other —C=O in other PLA backbone as mentioned FTIR spectra analysis. Several kinds of intermolecular hydrogen bonding could be formed with different LCB structure in product. The formation of intermolecular hydrogen bonding is schematically shown in Scheme 2(A)–(C). Such intermolecular hydrogen helps to form a cluster of polymer chains, which increases the local orientation order and can act as the nuclei for crystallization. Actually, the branching level in D2 is only slight larger than that in D1, while the intermolecular hydrogen bonding due to the grafting of PETA causes the nucleation much easier and crystallization speed becomes much faster.

CONCLUSIONS

In this study, we prepared long chain branching PLA by melt radicals reaction with PETA and DCP. The addition of PETA during melt radical reaction can introduce more branched structure, which is justified by the rheological experiments and the fitting results with the Branch-On-Branch model. Not only the fraction of comb-like chain increases but also the number of arm in the comb-like chain increases after the introduction of PETA. Moreover, it is found by FTIR that evident hydrogen bonding between PLA chains appears after the grafting of PETA. The cold crystallization was found to be easier due to the decrease in the crystallization temperature as the branch level increases. Further studies showed that the half crystallization time decreases substantially in PETA grafted PLA sample, and especially the crystallization rate constant k of D2 increases to around 1000 times of that of neat PLA at the same crystallization temperatures. The great enhancement in the crystallization rate of PETA grafted PLA is ascribed to the increase in the nucleation density, which in D2 is about 10 times as much as that of neat PLA. Such great improvement in the nucleation density is due to the formation of chain cluster in the presence of hydrogen bonding. By comparing two branched PLAs with strong hydrogen bonding, i.e., D2 and P-P02-T04, it suggests

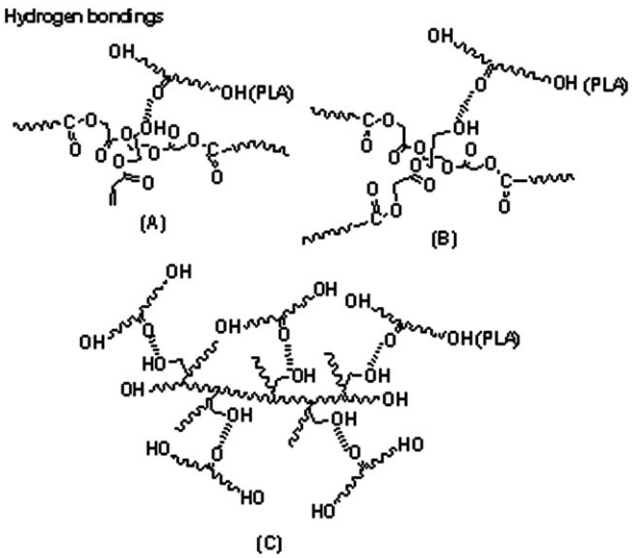

Scheme 2. The hydrogen bonding in the PETA grafted PLA sample D2.

that under the similar nucleation effect due to the hydrogen bonding interaction, highly branched structures like P-P02-T04 shows a slower crystallization speed due to the relatively low mobility of molecules. Therefore, introduction of PETA during melt radical reaction not only increases the level of long chain branching, which helps to promote the melt strength, but also accelerates the crystallization process.

ACKNOWLEDGMENTS

The authors would like to thank the support from National Basic Research Program of China (973Program) 2012CB025901 and the National Natural Science Foundation of China (No. 21074072). W. Yu is supported by the Program for New Century Excellent Talents in University and the SMC project of Shanghai Jiao Tong University.

REFERENCES

1. Leenslag, J. W.; Pennings, A. J.; Bos, R. R. M.; Rozema, F. R. *Biomaterials* **1987**, *8*, 311.
2. Tasaka, F.; Ohya, Y.; Ouchi, T. *Macromolecules* **2001**, *34*, 5494.
3. Bordes, P.; Pollet, E.; Averous, L. *Prog. Polym. Sci.* **2009**, *34*, 125.
4. Jalil, R. *Drug Dev. Ind. Pharm.* **1990**, *16*, 2353.
5. Leenslag, J. W.; Penning, A. J. *Polym. Commun.* **1987**, *28*, 92.
6. Baratian, S.; Hall, E. S.; Lin, J. S.; Xu, R. *Macromolecules* **2001**, *34*, 4857.
7. Cho, J.; Baratian, S.; Kim, J.; Yeh, F.; Hsiao, B. S. *Polymer* **2003**, *44*, 711.
8. Xu, H.; Teng, C. Q.; Yu, M. H. *Polymer* **2006**, *47*, 3922.
9. Martin, O.; Ave′rous, L. *Polymer* **2001**, *42*, 6209.
10. Shibata, M.; Teramoto, N.; Inoue, Y. *Polymer* **2007**, *48*, 2768.
11. Xiao, H. W.; Lu, W.; Yeh, J. T. *J. Appl. Polym. Sci.* **2009**, *113*, 112.
12. Xiao, H. W.; Li, P.; Ren, X. M.; Jiang, T.; Yeh, J. T. *J. Appl. Polym. Sci.* **2010**, *118*, 3558.
13. Schmidt, S. C.; Hillmyer, M. A. *J. Polym. Sci. Part B: Polym. Phys.* **2001**, *39*, 300.
14. Liao, R. G.; Yang, B.; Yu, W.; Zhou, C. X. *J. Appl. Polym. Sci.* **2007**, *104*, 310.
15. Xu, Z. H.; Niu, Y. H.; Yang, L.; Xie, W. Y.; Li, H.; Gan, Z. H.; Wang, Z. G. *Polymer*, **2010**, *51*, 730.
16. Xu, Z. H.; Niu, Y. H.; Wang, Z. G.; Li, H.; Yang, L.; Qiu, J.; Wang, H. *ACS Appl. Mater. Interfaces* **2011**, *3*, 3744.
17. Tachibana, Y.; Maeda, T.; Ito, O.; Maeda, Y.; Kunioka, M. *Polym. Degr. Stab.* **2010**, *95*, 1321.
18. Liang, W.; Zhong, X.; Dong, K. H. *J. Polym. Sci. Part B: Polym. Phys.* **2010**, *48*, 1235.
19. Zhang, J. F.; Sun, X. Z. *Biomacromolecules* **2004**, *5*, 1446.
20. Carlson, D.; Dubois, P.; Li, N.; Narayan, R. *Polym. Eng. Sci.* **1998**, *38*, 311.
21. Carlson, D.; Li, N.; Narayan, R.; Dubois, P. J. *Appl. Polym. Sci.* **1999**, *72*, 477.
22. Liu, J. Y.; Lou, L. J.; Yu, W.; Zhou, C. X. *Polymer* **2010**, *51*, 5186.
23. Wang, Y. B.; Niu, Y. H.; Yang, L.; Yu, F. Y.; Zhang, H. B.; Wang, Z. G. *Chem. J. Chinese U* **2010**, *31*, 397.
24. Wang, Y. B.; Yang, L.; Niu, Y. H.; Wang, Z. G.; Zhang, J.; Yu, F. Y.; Zhang, H. B. *J. Appl. Polym. Sci.* **2011**, *122*, 1857.
25. Wang, X. C.; Tzoganakis, C.; Rempel, G. J. *Appl. Polym. Sci.* **1996**, *61*, 1395.
26. Tian, J. H.; Yu, W.; Zhou, C. X. *J. Macromal. Sci. Part B: Phys.* **2006**, *47*, 7962.
27. Tian, J. H.; Yu, W.; Zhou, C. X. *J. Appl. Polym. Sci.* **2007**, *104*, 3592.
28. Younes, H.; Cohn, D. J. *Eur. Polym. J.* **1988**, *24*, 765.
29. Park, J. W.; Lee, D. J.; Yoo, E. S. *J. Korea Polym. J.* **1999**, *7*, 93.
30. Kister, G.; Cassanas, G. Vert, M. *Polymer* **1998**, *39*, 267.
31. Lagaron, J. M. *Macromol. Symp.* **2002**, *184*, 19.
32. Trinkle, S.; Friedrich, Ch. *Rheol. Acta* **2001**, *40*, 322.
33. Trinkle, S.; Walter, P.; Friedrich, Ch. *Rheol. Acta* **2002**, *41*, 103.
34. Liu, J. Y.; Yu, W.; Zhou, C. X. *J. Rheol.* **2011**, *55*, 545.
35. Das, C.; McLeish, T. C. B. *J. Rheol.* **2006**, *50*, 207.
36. Babanalbandi, A.; Hill, D. J. T.; O'Donnell, J. H. *Polym. Deg. Stab.* **1995**, *50*, 297.
37. Ouchi, T.; Ichimura, S.; Ohya, Y. *Polymer* **2006**, *47*, 429.
38. Liu, H.; Hu, D. *Polym. Bull.* **1994**, *32*, 463.
39. Yeh, J-t.; Huang, C.; Chai, W.; Chen, K. J. *Appl. Polym. Sci.* **2009**, *112*, 2757.
40. Hu, Y.; Zhang, J. M.; Sato, H.; Futami, Y.; Noda, I.; Ozaki, Y. *Macromolecules* **2006**, *39*, 3841.